Synthesis and Characterization of Novel Poly(acrylamide-*co*-acrylic acid-*co*-2-hydroxy ethyl actylate) Hydrogels: Mathematical Approach in Investigation of Swelling Kinetics and Diffusion Models

Seema Awasthi, Reena Singhal

Department of Plastic Technology, H. B. Technological Institute, Kanpur, Uttar Pradesh 208002, India

Received 12 February 2011; accepted 18 July 2011
DOI 10.1002/app.35288
Published online 26 October 2011 in Wiley Online Library (wileyonlinelibrary.com).

ABSTRACT: In this study, a series of poly(acrylamide-*co*-acrylic acid-*co*-2-hydroxy ethyl actylate) [AM-*co*-AA-*co*-HEA] hydrogels have been synthesized by varying the acrylic acid (AA)content over eightfold in feed in the range of 33.34–93.76% by keeping other monomer constant. These hydrogels were characterized by FTIR, SEM analysis, elemental analysis, residual acrylic acid analysis, network parameters, and dynamic swelling behavior. The swelling study showed that equilibrium swelling ratio was nonlinearly increased with increasing AA content. Interestingly, the equilibrium swelling ratio decreased from 53.42 to 48.52 for 75–80% AA content hydrogel. The swelling data were found to satisfactorily fit Fick's second law, demonstrating that diffusion rate of water uptake was primarily Fickian. From model fitting, it was observed that early model was applicable for first 30% water absorption, and late model was applicable for latter 70% water absorption for increasing AA content from 33.34–90.90%. For 93.76% AA, early-time model was extended up to first 50% of water absorption and late model was contracted for latter 50% water absorption, indicating that excessive AA content affects the applicability range of early-time and late-time diffusion models for water absorption. Etters model was best applicable to all type of hydrogels and followed over all swelling range. © 2011 Wiley Periodicals, Inc. J Appl Polym Sci 124: 2348–2361, 2012

Key words: Etters model; hydrogels; acrylic acid; media penetration velocity; network parameters

INTRODUCTION

Anionic polymeric networks formed by chemical or physical crosslinking of macromolecular chains are a special class of three-dimensional, crosslinked, bioresponsive hydrogels. Anionic hydrogels contain acidic (e.g., carboxylic or sulfonic acid) groups in their polymeric backbones. These hydrogels imbibe a large amount of water and respond to changes in the physiological condition.[1,2] The higher water concentration in the hydrogel aids compatibility with natural tissues. Hence, ionic hydrogels have found applications in novel controlled drug delivery devices and other biomedical systems.[3,4] Anionic networks have excellent potential as bioresponsive polymers because the magnitude of their response can be controlled by changing the charge density or nature of the ionic moieties in the polymer.

Equilibrium swelling ratio is a direct measure of swelling/diffusion rate of the water uptake into the hydrogel.[5] The solvent sorption rate indicates the solvent uptake per unit time. The swelling kinetic/drug release kinetic of hydrogel had been analyzed by various authors[6,7] using different types of kinetic models. Solvent diffusion into the hydrogel changes the glassy state of the hydrogel network to the rubbery state, and moving the solvent boundary in the hydrogel is characterized by a media penetration velocity. Water induces a plasticizing effect in the hydrogel, thereby increasing the segmental movements as well as enlarging the mesh size of hydrogel network. This enlarge mesh size facilitates the drug diffusion through the rubbery matrix to the external medium, and the drug release depends upon the degree of swelling.

The measurement of diffusion in hydrogels has received considerable attention since the nature of water transport is of paramount importance for a proper understanding of transport phenomena of solutes through the hydrogels. Generally, most approximation equations are found to be only applicable to either the early stage or late stage of water diffusion.[8,9] Several efforts[10–12] have been made to illustrate the entire media diffusion profile. However, the "Etters model approximation equation"[13] is

Correspondence to: R. Singhal (reena_singhal123@rediffmail.com).

a semiempirical equation derived from a statistical regression of solute diffusion profiles and presents the analytical solution of the entire drug releases profile along with media diffusion to within 2% error.[14] Therefore, this model is used for both media diffusion and drug diffusion.

To evaluate the network parameters, a large number of modified equations for different cases have been used as summarized in literature.[6,15–25] Molecular weight between crosslink (M_c) is an important structural parameter characterizing the crosslink density (q) as well as mesh size (ξ). This parameter M_c is directly proportional to the mesh size whereas inversely proportional to the crosslinked density. Its magnitude significantly affects the physical properties of hydrogel. The degree of swelling is an important parameter; which is directly proportional to the mesh size, number-average molecular weight between crosslinks, whereas crosslinking density followed inverse trend with extent of swelling.[26] In ionic hydrogels, network parameters may be controlled by the monomer concentration in the reacting polymerization solution and by the swelling solution pH.

Now, an attempt is made to tailor the copolymeric hydrogel (having the same monomers with varying compositions) for different swelling, diffusion, and network parameters for different applications. The three monomers, acrylamide (AM), acrylic acid (AA), and 2-hydroxy ethyl acrylate, were selected in this study for the following reasons. AM [24] was chosen because of its biocompatible nature, permeable to oxygen, and higher water absorbing capacity. AA [22] was used as a comonomer as it exhibits smart nature, structural similarity with AM, and has a carboxylic group, which makes it highly hydrophilic. Hydrophilic monomer 2-hydroxy ethyl acrylate[16] is used to prevent hydrogel solubilization at high AA content and to develop mechanical properties.

AA variation has been studied for various hydrogels having a combination of hydrophilic and hydrophobic monomers[21,22,27–30] in the lower ranges from 10 to 70% and usually an increasing trend in swelling was observed. As synthesis of hydrogels based on AA, AM, and 2-hydroxy ethyl acrylate is not reported, we synthesized a series of poly(acrylamide-*co*-acrylic acid-*co*-2-hydroxy ethyl acrylate) [poly(AM-*co*-AA-*co*-HEA)]-based hydrogels having AA in very high ranges from 33.34 to 93.76%. The final incorporation of AA in resulting hydrogel was determined, and effect of variation in AA content on swelling and diffusion kinetics was evaluated using mathematical models. Swelling results were used to characterize the network parameters to get an insight into the effect of AA content on hydrogel structure and thus, finally to observe their effect on dynamic swelling behavior for controlling the water uptake. The swelling mechanism and diffusion process were determined through the use of "early-time," "late-time," and "Etters" approximation derived from a simple approximation model based on Fick's second law capable of describing the entire range of diffusion process.

EXPERIMENTAL

Materials

Acrylic acid (AA), acrylamide (AM), ammonium per sulfate (APS), and sodium hydroxide (NaOH) were procured from Central Drug House, New Delhi, India. Methanol was purchased from Qualikems, New Delhi. 2-Hydroxy ethyl acrylate (HEA) along with glycidyl methacrylate (GMA) were obtained from Aldrich Chemical Company, USA. AM was recrystallized from methanol before use. Sodium hydroxide (34.5%) solution was used to obtain the 75% neutralization of AA up to 4.5 pH. Double glass distilled water was used in all the experiments.

Polymerization procedure of poly(AM-*co*-AA-*co*-HEA) hydrogels

The polymerization of AM, AA, and HEA monomer was carried out into a three-necked flask equipped with a two blade stirrer, a reflux condenser, and a nitrogen inlet. The actual feed compositions for synthesis of poly(AM-*co*-HEA-*co*-AA) hydrogels by varying the AA content over eightfold by solution polymerization are given in Table I. The weight ratios of AM/AA/HEA monomers used in synthesis of hydrogels were 1/1/1, 1/2/1, 1/4/1, 1/6/1, 1/8/1, 1/10/1, 1/20/1, and 1/30/1, and the resulting hydrogels were designated as RK_1, RK_2, RK_3, RK_4, RK_5, RK_6, RK_7, and RK_8, respectively. In the synthesis of chemically crosslinked poly(AM-*co*-AA-*co*-HEA) hydrogels, the solution of monomers was prepared by adding 60 mL distilled water and monomers (AM, 2-hydroxyethyl acrylate, and AA) as per requirement based on weight ratio (Table I) to a beaker. This solution was then poured into a three-necked flask. Subsequently, the crosslinker, 0.1 g GMA (1% by weight of total monomer), was added into a three-necked flask. The three-necked flask was immersed in a thermostat oil bath. After being purged nitrogen for 15 min to remove the oxygen, the reaction mixture was mixed with the help of mechanical stirrer for complete dissolution and stirred vigorously for 3 h in a thermostat oil bath at 60°C temperature. In this solution, the initiator, 0.1 g APS (1% by weight of total monomer), which was dissolved in 6 mL distilled water, was introduced into the flask. For homogeneity, this reaction mixture was again stirred under nitrogen atmosphere for 2 h at 60°C. The resulting solution was then poured into

TABLE I
Various Feed Compositions Used for the Preparation of Poly (AM-*co*-AA-*co*-HEA) Hydrogels by Varying AA Over 30-Fold

Hydrogel code	Weight ratio of monomer composition in the Hydrogel AM/AA/HEA	Ratio in percentage AM/AA/HEA	Amount of AM (g)	Amount of AA (g)	Amount of HEA (g)
RK_1	1/1/1	33.33/33.34/33.33	3.333	3.334	3.333
RK_2	1/2/1	25.00/50.00/25.00	2.50	5.00	2.50
RK_3	1/4/1	16.67/66.66/16.67	1.667	6.666	1.667
RK_4	1/6/1	12.50/75.00/12.50	1.25	7.50	1.25
RK_5	1/8/1	10.00/80.00/10.00	1.00	8.00	1.00
RK_6	1/10/1	08.33/83.34/08.33	0.833	8.334	0.833
RK_7	1/20/1	04.55/90.90/04.55	0.455	9.090	0.455
RK_8	1/30/1	03.12/93.76/03.12	0.312	9.376	0.312

Petri dishes and kept for 2 h in a hot air oven at 60°C for polymerization and subsequent crosslinking. After the completion of reaction in 2 h, the firm hydrogel, in the form of thick sheet, was carefully removed from the surface of Petri dishes. Thereafter, separation of unreacted monomers is done by swelling and washing for 4 h in distilled water for three times. The resultant hydrogel sheet was cut into small pieces (1–2 cm), which were dried in an oven at 60°C up to the constant weight. The dried hydrogel was stored in desiccators. To eliminate the factor of experimental error, for each hydrogel, the polymerization experiment was repeated three times. The chemical reaction occurring during solution polymerization of AM, AA, and HEA monomer has been shown in Figure 1.

Characterization of hydrogel

Fourier transform infrared spectroscopy

The FTIR spectra of poly(AM-*co*-AA-*co*-HEA) hydrogels were recorded on a Bruker Spectrophotometer (Vertax 70) using solid pellet potassium bromide.

Chemical composition

The chemical composition in various resulting hydrogel was determined through the techniques as given below in following section.

Elemental analysis. Elemental analysis for nitrogen was performed on an Elemental Analyzers (Elemental Vario EL III Carlo Erba 1108).

Residual AA estimation. Elemental analysis was not suitable in calculating the percentage of AA and HEA due to the presence of same elements like C, H, and O in both. Therefore, the amount of AA present in water after washing of hydrogel was estimated on the basis of acid–base titration method[28] using phenolphthalein indicator. In this process, a known quantity of synthesized hydrogels was washed in distilled water till it reaches equilibrium, and the remaining unreacted AA in wash water was estimated with a standard 0.01*N* NaOH solution. Thereafter, unreacted AA was subtracted from originally taken in feed to calculate the exact AA in resulting hydrogel. The HEA % content was calculated on the basis of subtraction of (AA + AM) content from total, i.e., 100.

Differential scanning calorimetry

Differential scanning calorimetry (DSC) analysis was carried out using a Perkin–Elmer (Pyris Diamond) differential scanning calorimeter under the nitrogen atmosphere at a heating rate of 10°C/min from 35 to 200°C.

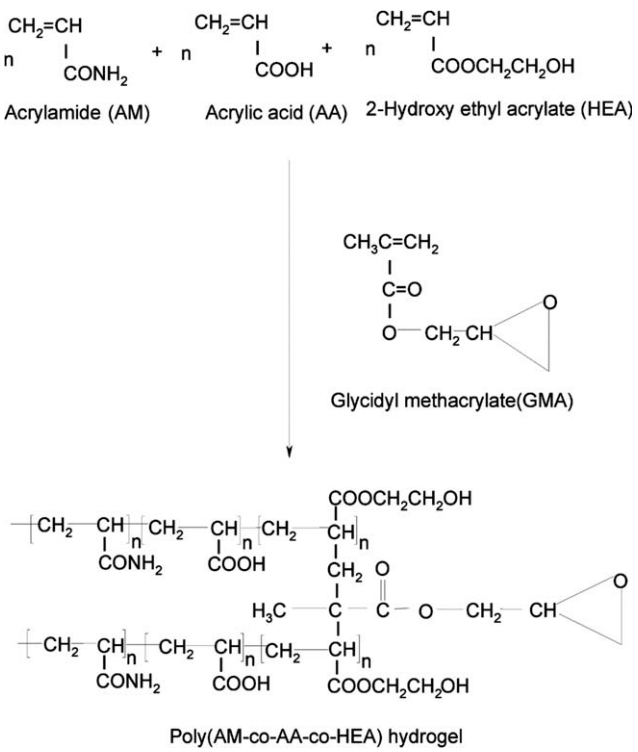

Figure 1 Scheme for synthesis of poly(AM-*co*-AA-*co*-HEA) hydrogel.

Scanning electron microscopy

The morphology of a synthesized poly(AM-*co*-AA-*co*-HEA) hydrogel surface was examined under a scanning electron microscope (SEM). Dried hydrogels coated with a thin layer of pure gold, i.e., 5150-sputter coater, and imaged in SEM (FEI QUANTA 2000).

Dynamic swelling behavior

This study is conducted to analyze the result of dynamic swelling properties as a function of AA content. The dynamic swelling properties such as swelling ratio, transport mechanism, swelling rate, and media penetration velocity for the controlling solvent sorption are discussed in the following section given below.

Extent of swelling study

Conventional gravimetric procedure[29] was adopted for studying the extent of swelling in 500 mL distilled water. The swelling ratio was calculated by eq. (1)

$$\text{Swelling ratio } '\Phi' = \frac{W_s}{W_d} \tag{1}$$

where W_s and W_d are the weights of the water-swollen hydrogel and dry hydrogel, respectively.

Transport mechanism

The diffusion mechanism, which indicates the relative importance of diffusion and relaxation, is typically determined by fitting sorption data (for short time or $M_t/M_\infty \leq 0.6$) to the empirical power law expression proposed by the Ritger and Peppas.[31,32]

$$\frac{M_t}{M_\infty} = k\, t^n \tag{2}$$

where M_t is mass of water absorbed at time t, M_∞ is the mass of water absorbed at equilibrium, M_t/M_∞ is the fractional water absorbed, k is constant characteristic of water absorbed, and "n" is the diffusion exponent and denotes the type of diffusion mechanism. When $n = 0.50$, the process is diffusion controlled and is termed Fickian or case I. Diffusion is assumed to be relaxation-controlled (Case II) when $n = 1$. Non-Fickian or anomalous diffusion occurs when the exponent "n" is between 0.50 and 1.0.

Swelling kinetics

Swelling rate constant gives an idea about the swelling kinetics of the hydrogels and tells about the speed of entering water into the hydrogel, through which hydrogel can swell faster or slow rate. The second-order swelling kinetic theory assumes that the swelling rate of a hydrogel is controlled by both the diffusion of solvent molecules and the relaxation of macromolecule chains. The second-order swelling kinetics[33] can be described as indicated in eq. (3)

$$\frac{dH}{dt} = K_r(H_\infty - H)^2 \tag{3}$$

where K_r is swelling rate constant, H is the degree of swelling at time t, and H_∞ is the degree of swelling at equilibrium. Degree of swelling was calculated according to the equation given in literature.[34]

By integration of eq. (3), and applying the initial conditions, we have eqs. (4) and (5):

$$\frac{t}{H} = \frac{1}{K_\infty} + \frac{t}{H_\infty} \tag{4}$$

$$K_\infty = K_r x H_\infty \tag{5}$$

Here, K_∞ is the equilibrium swelling rate constant.

The well-known Schott's equation (4) is a linear relationship, and H_∞ and K_r correspond to the slope and intercept of the straight line, respectively.[35]

The rate, at which the glassy to rubbery front advanced from the surface to the center of the hydrogel disk, was determined by the media penetration velocity. The penetration velocity for each hydrogel was determined by the weight gain method as described by Peppas.[36,37] The penetration velocity was calculated using eq. (6):

$$u = \frac{1}{2\rho A^*}\frac{\partial W_g}{\partial t} \tag{6}$$

where u denotes the penetration velocity, $\partial W_g/\partial t$ denotes the slope of the weight gain versus time curve, ρ denotes the density of water at room temperature, and A^* denotes the area of the one face of the disk. In this study, length of disk was $\sim$ 1.4–1.3 cm, width of disk was $\sim$ 0.9–0.8 cm, and thickness of disk was 1 cm.

Network parameter studies

Network parameters, i.e., the number-average molecular weight between crosslinks (M_c), crosslinking density (q), and mesh size (ξ), were determined to focus their impact on the dynamic swelling behavior for controlling the water uptake as a function of AA content.

The modified anionic equation (7) for calculation of M_c in anionic hydrogels is given below.[18]

$$\frac{V_1}{4IM_r}\left(\frac{V_s}{v}\right)^2\left(\frac{K_a}{10^{-\mathrm{pH}}+K_a}\right)^2 = (\ln(1-V_s)+2V_s+\chi V_s{}^2) + \left(\frac{V_1}{vM_c}\right)\left(1-\frac{2M_c}{M_n}\right)V_r\left\{\left(\frac{V_s}{V_r}\right)^{1/3}-\left(\frac{V_s}{2V_r}\right)\right\} \quad (7)$$

In this expression, V_1 is the molar volume of water, M_n is molecular weight of the polymer chains prepared under identical condition but in the absence of the crosslinking agent (1.15×10^5), ν is the specific volume of the polymer, and V_s is the polymer volume fraction in the swollen state, i.e., equal to reverse of swelling ratio "Φ".[38] V_r is polymer volume fraction in the relaxed state, which is defined as the state of the polymer immediately after crosslinking, but before swelling. V_r was calculated according to the method reported by Okay and Durmaz.[39] I is the ionic strength of the swelling medium ($I = 1 \times 10^{-4}$ mol mL^{-1}). The reported value of acid dissociation constant ($K_a = 5.6 \times 10^{-5}$) is taken from the literature.[5] The molar volume of water at 25°C is 18 cm^3 mol^{-1}. The molecular weight of the repeating unit of hydrogel "M_r" is calculated according to Hariharan and Peppas.[40] Flory–Huggins interaction parameter "χ" between solvent and polymer is calculated according to the method proposed by Xue et al.[41]

The crosslink density "q" is defined as the mole fraction of crosslinked units.[42]

$$q = \frac{M_o}{M_c} \quad (8)$$

where M_o is the molar mass of the repeating unit and can be calculated by the following eq. (9).

$$M_o = \frac{M_r}{n\mathrm{AM} + n\mathrm{AA} + n\mathrm{HEA}} \quad (9)$$

where, nAM, nAA, and nHEA are mole numbers of AM, AA, and HEA monomer, respectively.

Assuming isotropic swelling of the hydrogel and using the Flory characteristic ratio "C_n" for calculation of the end-to-end distance, the mesh size of a swollen hydrogel network can be calculated using eq. (10).[18]

$$\xi(\text{Å}) = \left[\frac{2C_nM_c}{M_r}\right]^{1/2} l\, V_s{}^{-1/3} \quad (10)$$

where ℓ is the carbon–carbon bond length (1.54 Å), and the value of Flory characteristic ratio "C_n" is 6.32.

Modeling of the diffusion process and determination of diffusion coefficient

Analysis of the water diffusion process for various poly(AM-*co*-AA-*co*-HEA) hydrogels was carried out using the "early-time" model [eq. (13)],[32,36] the "late-time" model [eq. (14)],[32,36] and the "Etters" model [eq. (15)],[13] respectively. These models used to describe the diffusion process in this work were based on solutions of Fick's second law,

$$\frac{\partial C}{\partial t} = D\frac{\partial^2 C}{\partial x^2} \quad (11)$$

subject to the following initial and boundary conditions

$$t = 0, -\frac{\delta}{2} < x < \frac{\delta}{2}, c = 0; t > 0, x = 0,$$
$$\frac{\partial c}{\partial x} = 0; t > 0, x = \pm\frac{\delta}{2}, c = 0$$

where c is the concentration of solute, t is time, x is position in the hydrogel, δ is the total thickness of the hydrogel sheet, and D is diffusion coefficient. This assumes diffusion in one dimension with constant boundary conditions.[43] The solution to this equation is an infinite series,

$$\frac{M_t}{M_\infty} = 1 - \sum_{n=0}^{\infty}\frac{8}{(2n+1)^2\pi^2}\exp\left[\frac{-D(2n+1)^2\pi^2 t}{\delta^2}\right] \quad (12)$$

where M_t is the mass of water in hydrogel at any time t, and M_∞ is the mass of water in hydrogel at long times when the hydrogel has reached equilibrium.

The "early-time" eq. (13), the "late-time" eq. (14), and the "Etters" eq. (15) are three well-accepted approximations of eq. (12). These models have been used to better understand the modeling of the diffusion process and their applicability range for diffusion process. Generally, early-time approximation applies for the first 60% of water absorption and the late-time approximation applies for the latter 40% water absorption, whereas Etters model is valid for over all range of water absorption. These models were used to determine the diffusion coefficients for both media diffusion and solute diffusion.

$$\frac{M_t}{M_\infty} = 4\left[\frac{D_i t}{\pi\delta^2}\right]^{0.5} \quad (13)$$

$$\frac{M_t}{M_\infty} = 1 - \frac{8}{\pi^2}\exp\left[\frac{-D_L\pi^2 t}{\delta^2}\right] \quad (14)$$

$$\frac{M_t}{M_\infty} = \left[1 - \exp\left(-K\left(\frac{D_E t}{\delta^2}\right)^a\right)\right]^{1/b} \quad (15)$$

Here, D_i is early diffusion coefficient, D_L is late diffusion coefficient, and D_E is Etters diffusion coefficient. For the Etters model, a, b, and k were 1.3390, 2.6001, and 10.5449, respectively. δ is the thickness of the hydrogel.

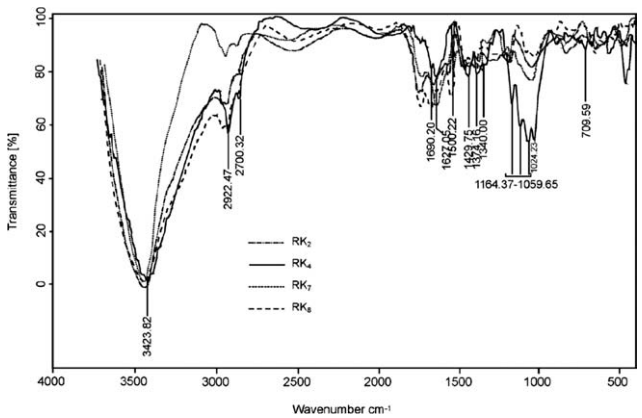

Figure 2 FTIR spectra of poly(AM-*co*-AA-*co*-HEA) hydrogels containing 50%, 75%, 90.90%, and 93.76% AA content for characterizing the RK2, RK4, RK7, and RK8 hydrogels.

For a process controlled by diffusion in thin disks, a complementary method for the early-time approximation is a power law expression (eq. 2)[31,32] to determine the nature of diffusion. The proportionality constant (k) can be used to calculate the diffusion coefficient, and n denotes the type of diffusion mechanism. When $n = 0.50$, the diffusion rate is Fickian (as was assumed for an early-time approximation equation). To avoid any discrepancies, for each hydrogel, all experiments were done in triplicate and results averaged. For modeling of the diffusion process, the average of values for "D" and "n" is reported along with standard deviation in Table III.

RESULTS AND DISCUSSION

Spectral analysis

Fourier transform infrared spectroscopy (FTIR) was used to analyze the synthesized RK_2, RK_4, RK_7, and RK_8 hydrogels, and the results are shown in Figure 2. The highest peak at 3423.82 cm^{-1} is corresponding to —NH stretching of the amide group of AM. The peaks at 2922.47 cm^{-1} and 1429.75 cm^{-1} indicate the presence of alkane. A small peak at 2700.32 cm^{-1} is an indication for O—H stretching of —COOH group. The characteristic peak at 1500.22 $cm^{-1}$was attributed to C=O asymmetric stretching in the carboxylate anion. This was confirmed by another peak at1374.16 cm^{-1}, which is related to the symmetric stretching made of the COO^- (carboxylate ion) groups. The peaks at 1690.20 and 1627.05 cm^{-1} are attributed to —C=O stretching (amide I band) and —NH stretching (amide II band), respectively, while peak at 1340 cm^{-1} can be attributed to —C—N stretching (amide III band). The peak at 1024.23 cm^{-1} is an indication to —O—C stretching of $—CH_2OH$ moiety. In addition to the above, few peaks at 1164.37–1059.65 cm^{-1} are also observed corresponding to —C—O—C— stretching interactions of ester groups, and peak at 709.59 cm^{-1} is an indication of methylene rocking. It is observed that the peaks at 2700.32, 1500.22, and 1374.16 cm^{-1} were found to be shifted to lower frequencies as the results of more absorption during the increased concentration of AA content. FTIR analysis indicates that all monomer units (AM, 2-HEA, and AA) were incorporated into hydrogel.

Determination of chemical composition of hydrogel

AM content in synthesized hydrogels was determined through elemental analysis for N element, and the results are given in Table II. AA content was determined through extraction analysis, and the remaining HEA content for RK_1 to RK_8 hydrogels is given in Table II. It can be seen from Table II that for RK_1 hydrogel, 33.33% AM was taken in feed, but 38.44% AM was found to be present in resulting hydrogel indicating higher amount of AM being incorporated. Similar trend was followed in all resulting hydrogel from RK_2 to RK_8. However, an interesting exception was observed for RK_5 hydrogel where AM in feed was 10%, but 19.37% AM was incorporated in resulting hydrogel, indicating

TABLE II
Results for Calculated Composition Analysis of Synthesized Hydrogels RK_1 to RK_8 Along with Percentage Taken in Feed

		%AM		%AA		%HEA	
Hydrogels code	% of N element (determined by elemental analysis)	Taken in feed	Present in resulting hydrogels	Taken in feed	Present in resulting hydrogels	Taken in feed	Present in resulting hydrogels
RK_1	7.58	33.33	38.44	33.34	33.25	33.33	28.31
RK_2	6.09	25.00	30.88	50.00	48.85	25.00	20.27
RK_3	4.17	16.67	21.15	66.66	65.48	16.67	13.37
RK_4	3.15	12.50	15.97	75.00	74.77	12.50	9.26
RK_5	3.82	10.00	19.37	80.00	70.16	10.00	10.47
RK_6	2.35	8.33	11.92	83.34	82.24	8.33	5.84
RK_7	1.95	4.55	9.89	90.90	86.59	4.55	3.52
RK_8	1.12	3.12	5.68	93.76	92.24	3.12	2.08

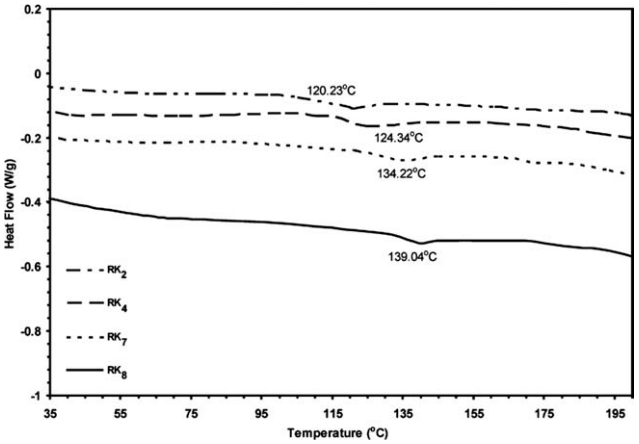

Figure 3 DSC thermogram of poly(AM-*co*-AA-*co*-HEA) hydrogels RK2, RK4, RK7, and RK8 containing acrylic acid content 50%, 75%, 90.90%, and 93.76%, respectively.

that exceptionally high AM was being incorporated into the resulting hydrogel. The AA content in synthesized hydrogel for RK_1 to RK_8 was approximately same to the AA taken in feed. However, in case of RK_5 hydrogel that contains 80% AA in feed, only 70.16% AA was found to be present in resulting hydrogel, leading to very low AA content in resulting hydrogel. A total of 33.33–25% HEA content was taken in feed for RK_1 to RK_2, and 28.31–20.27% HEA content was found in synthesized hydrogel showing 5% difference, which was comparatively low pronounced in resulting hydrogel. For RK_3, RK_4, and RK_6 hydrogels, this difference was 3%. For RK_5 hydrogel, 10% HEA was present in feed, but 10.47% HEA was contained in resulting hydrogel, leading to approximately same HEA was being incorporated in resulting hydrogel. The HEA content was further $\sim$ 1% less in resulting hydrogel for RK_7 to RK_8.

DSC analysis

The glass transition temperature (T_g) of poly(AM-*co*-AA-*co*-HEA) hydrogels (RK_2, RK_4, RK_7, and RK_8) having different amounts of AA content was determined by the DSC analysis, and the results are shown in Figure 3. The "T_g" values of RK_2, RK_4, RK_7, and RK_8 hydrogel were found to be 120.23, 124.34, 134.22, and 139.04°C, respectively. It is clear from the "T_g" value that by increasing the amount of AA content from 50 to 93.76%, the T_g increased from 120 to 139°C. This increase in "T_g" is due to its highly ionic nature of AA, which provided increased intermolecular interaction of acid groups.[22]

Effect of AA on dynamic swelling behavior

Effect of AA content on swelling extent

Equilibrium swelling ratio for RK_1 to RK_8 hydrogels by varying AA content from 33.34 to 93.76% is given in Table III. The AA when increased three times for RK_1 to RK_8 hydrogels resulted in increasing swelling ratio (Φ) more than four times, as depicted in Table III. However, swelling ratio dropped down when AA content was increased from 75 to 80% for RK_4 to RK_5 hydrogels. It is shown from Table III that as the AA content approaches to the double from 33.34 (RK_1) to 66.66% (RK_3), initially there was a marginal increase in equilibrium swelling ratio from 24.52 to 30.42. However, when AA content was raised from 66.66% (RK_3) to 75% (RK_4), equilibrium swelling ratio drastically increased from 30.42 to 53.42. The increase in equilibrium swelling ratio with increasing AA content implied that increasing the proportion of hydrophilic $-COO^-$ group in the hydrogel increased the affinity for water. The electrostatic repulsion between $-COO^-$ groups increases the osmotic pressure inside the polymer matrix and causes further expansion of the three-dimensional polymer network. To explain the above increased swelling behavior, fractured surface microstructure of hydrogels RK_2 and RK_4 before swelling was characterized by SEM. The RK_2 hydrogel [Figure 4 (a)] showed some roughness with heterogeneities and cracks, whereas RK_4 hydrogel showed increased surface area with channels and cracks [Figure 4 (b)]. It is clear from Figures 4(a,b) that RK_2 has comparatively regular and nonporous structure due to which lowest swelling ratio (26.04) was observed, but in RK_4 the microstructure is porous and containing channels due to which the swelling ratio got almost doubled (53.42).

However, a decrease in equilibrium swelling ratio from 53.42 to 48.52 was observed for hydrogels RK_4 to RK_5 having varying AA content from 75 to 80% in feed. The increasing content of AA in RK_5 hydrogel leads to a marked decrease in equilibrium swelling ratio, as given in Table III. This is possibly due to the decreased repulsion force of the carboxylate groups between polymeric network chains created by incorporation of only 70% AA content in synthesized hydrogel RK_5 than those taken in feed, where AA content was 80%. Because of decreased repulsion force of the carboxylate groups between polymeric network chains, the osmotic pressure difference between network chains decreases and ultimately causes decreased volume. As a result, swelling ratio decreased for resulting hydrogel RK_5. Apart from this, it is also clear from Table II that decreasing swelling ratio in RK_5 hydrogel was not only due to the incorporation of lower AA content in synthesized hydrogel but also due to the increased AM and HEA content. As observed in literature[34] that with increasing AM content the number of hydrophilic crosslinked poly(AM) chains increased greatly, which produce increased crosslink density. Therefore, because of denser networks

TABLE III
Results of Dynamic Swelling Studies; Network Parameter Study and Various Diffusion Coefficients for Early-Time, Late-Time and Etters Approximation for RK_1 to RK_8

	Dynamic swelling behavior						Network parameters			Diffusion coefficients (cm^2/min)					
				Peppas model						Early-time approximation		Late-time approximation		Etters approximation	
Hydrogel code	Equilibrium swelling ratio 'Φ'	Swelling Rate constant '$K_r \times 10^{-6}$'	Media penetration velocity '$u \times 10^{-3}$' (cm/min)	Diffusion exponent 'n'	Standard deviation	Gel characteristic constant '$K \times 10^{-2}$' ($min^{-0.5}$)	Average molecular weight between crosslink '$M_c \times 10^4$' (g/mol)	Crosslink density '$q \times 10^{-3}$' (mol/cm^3)	Mesh size '$\xi \times 10^2$' (Å)	$D_i \times 10^{-5}$	Standard deviation ($\times 10^{-5}$)	$D_L \times 10^{-5}$	Standard deviation ($\times 10^{-5}$)	$D_F \times 10^{-5}$	Standard deviation ($\times 10^{-5}$)
RK_1	24.52	42.8	17.6	0.52	±0.004	1.38	0.654	33.10	0.87	4.24	±0.22	7.10	±0.28	7.21	±0.034
RK_2	26.04	39.4	18.4	0.52	±0.003	1.43	3.070	4.69	2.37	4.13	±0.19	8.11	±0.32	7.21	±0.024
RK_3	30.42	38.9	20.4	0.51	±0.007	1.60	20.400	0.53	7.42	3.85	±0.21	5.07	±0.24	5.33	±0.036
RK_4	53.42	19.6	37.5	0.59	±0.004	0.90	26.300	0.36	10.5	4.42	±0.18	7.10	±0.20	5.33	±0.042
RK_5	48.52	20.4	35.1	0.56	±0.006	1.03	5.120	1.69	5.06	4.07	±0.22	6.09	±0.24	5.33	±0.055
RK_6	61.13	18.5	41.5	0.55	±0.004	1.17	5.430	1.66	5.25	3.79	±0.17	6.09	±0.26	5.33	±0.023
RK_7	65.43	17.6	44.3	0.55	±0.005	1.20	5.590	1.42	5.86	3.79	±0.17	5.07	±0.23	5.33	±0.032
RK_8	85.22	9.12	62.7	0.59	±0.002	0.81	5.680	1.35	6.55	4.24	±0.14	5.07	±0.24	5.33	±0.023

All values listed are the average of three experiments.

formation in the RK_5 hydrogel, the penetration of water molecules into the hydrogel becomes difficult, and this brought about a reduction in the equilibrium swelling ratio. In addition to above, according to Flory's ionic swelling theory,[38] HEA is nonionic in nature. As a result, the —OH group of HEA does not dissociate during the swelling; thus, the amount of dissociated ions inside the hydrogel decreases when the HEA content increases into the hydrogel. Because of this reason, with increasing HEA content, osmotic pressure difference between hydrogel chains decreases during the swelling. Accordingly, increased HEA content is further responsible for decreased swelling ratio in RK_5 hydrogel. These facts are in agreement with the result observed in SEM of RK_5 hydrogel [Figure 4(c)]. The fractured surface microstructure of hydrogels RK_5 [Figure 4(c)] showed a smooth and denser surface with somewhere very few bead-like formation due to which the swelling ratio decreased than RK_4-containing channels like structure. To verify the above fact, network parameters will be determined later.

Furthermore, the equilibrium swelling ratio again increased from 48.52 to 85.22 for RK_5 to RK_8 hydrogel comprised of 80–93.76% AA content. SEM images of RK_7 and RK_8 are shown in Figures 4(d,e), and it has been observed that both hydrogels have similar microstructure, which is highly porous and contain granular structures. The only difference is for RK_8 having smaller grain size and more porous structure leading to higher swelling ratio (85.22). The hydrogels having AA content more than 93.76% were not used in swelling studies as it got solubilized during swelling study, may be due to generation of excessive hydrophilic groups (—COO^-, —$CONH_2$, and —OH).

Figure 5 shows swelling ratios versus time plot at different swelling times (from 64 to 4356 min) for RK_1 to RK_8 hydrogels. It is clear from Figure 5 that the swelling is slow during the first 100 min. It indicates that initial swelling process is slow, mainly due to primarily slow water penetrating into the hydrogel through capillary and diffusion in the glassy state. Then, swelling is fast up to 1521 min because penetrated water is absorbed by hydrophilic groups such as carboxylate, amido and hydroxyl ethyl carboxylate through the formation of hydrogen bonds. The swelling is driven by repulsion of hydrophilic groups inside the network and osmotic pressure difference between the hydrogel and the external solution. Thus, subsequently, swelling gradually slows down until the swelling reaches up to equilibrium. As the AA content increased from RK_1 to RK_8 hydrogel, the swelling increased gradually except the RK_5 hydrogel. For RK_5 hydrogel, the AA content in resulting hydrogel was found to be significantly lower, i.e., 70% indicating higher HEA and

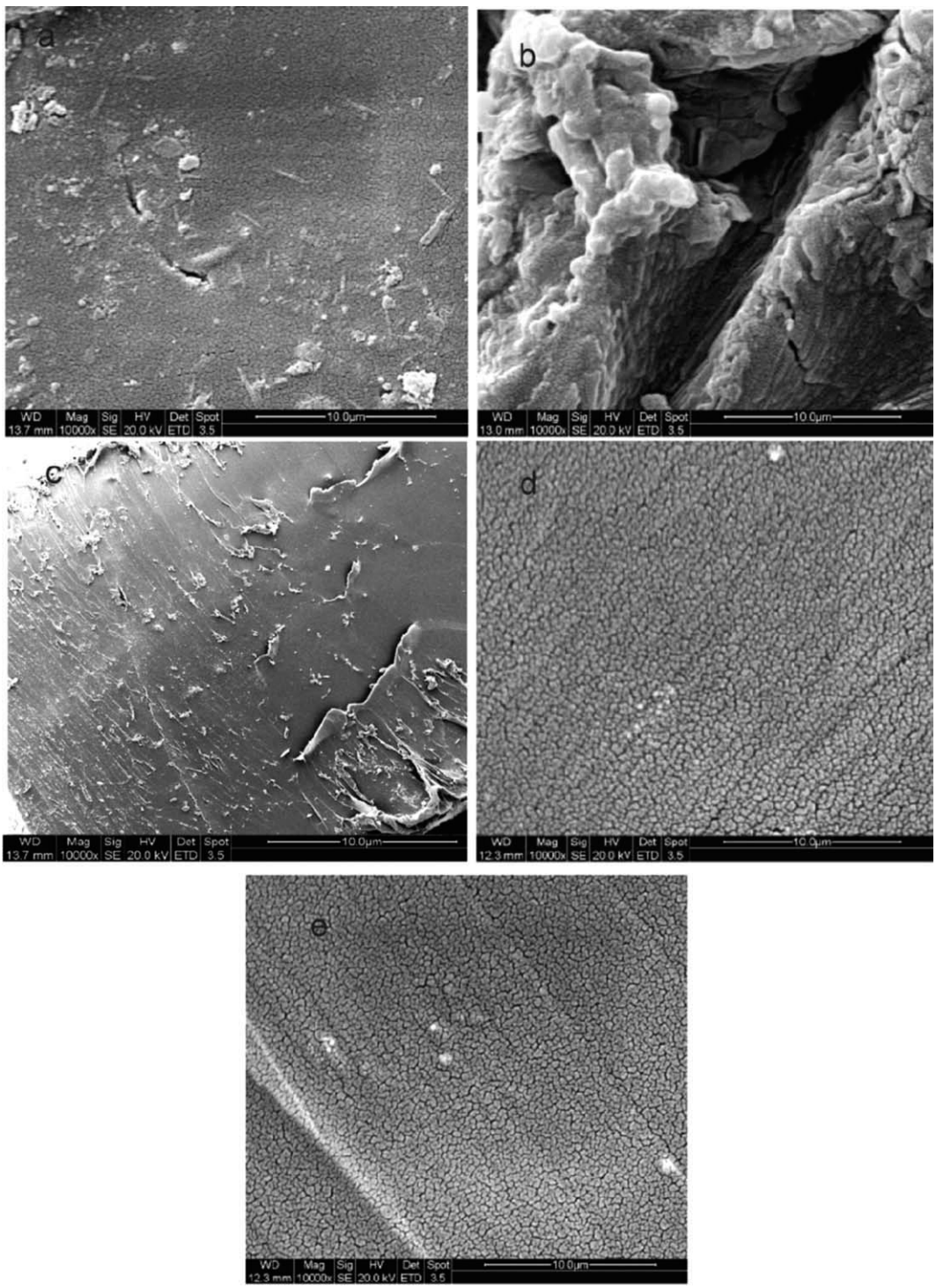

Figure 4 SEM micrograph of fractured surface of poly(AM-*co*-AA-*co*-HEA) hydrogels containing acrylic acid content (a) 50%, (b) 75%, (c) 80%, (d) 90.90%, and (e) 93.76%.

AM content. This led to lower hydrophilicity in the hydrogel and subsequently low swelling.

Wang et al.[30] have studied poly(AM-*co*-AA) hydrogel modified with hydroxyl propyl acrylate. They found that swelling ratio increased from 15 to 40 when the AA content increased from 19 to 55%. However, as AA content increased to the extent of 60%, a decreased swelling ratio from 40 to 25 was observed.

Effect of AA on the swelling mechanism

The swelling mechanism was analyzed by plotting data log M_t/M_∞ verses log t with the help of eq. (2).

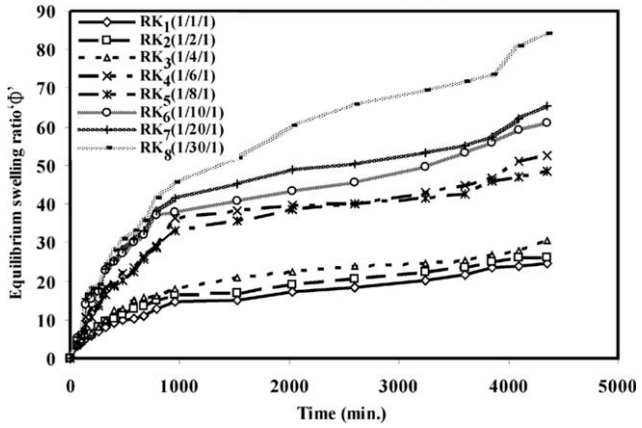

Figure 5 A plot between swelling ratio vs. time of swelling for poly(AM-*co*-AA-*co*-HEA) hydrogels comprised of 33.34%–93.76% acrylic acid (AA) content to observe the effect of acrylic acid content on equilibrium swelling ratio as a function of time.

The experimental data of swelling from the glassy hydrogels were fitted in equation to calculate the transport exponent (n) and characteristic constant of solvent absorbed (k). The results of these fitting are given in Table III. In all cases, experiments in triplicate were conducted for each hydrogel; and Table III shows the average value of "n" along with standard deviation. A very low value of standard deviations in value of "n" indicates that three n values were almost equivalent. As clear from the Table III, the value of swelling exponent (n) lies in the range of 0.51–0.59 for RK_1 to RK_8 hydrogels, and it can be taken nearly "0.5." Therefore, it can be stated that all hydrogels exhibit Fickian diffusion (diffusion-controlled) with increasing AA content. The values of k lie in the range of 0.81×10^{-2}–1.60×10^{-2}. Mullarney et al.[11] had reported similar "n" values for copolymeric hydrogels based on *N*,*N*-dimethylacrylamide (DMA) modified with hydrophobically 2-(*N*-ethylperfluoro octane sulfonamide) ethyl acrylate (FOSA) containing different amounts of FOSA. They found that the values of "n" lie in the range of 0.52–0.63.

Effect of AA on swelling kinetic and penetration velocity

Figure 6 shows the effect of AA content on dynamic swelling parameters such as swelling rate constant (K_r) and media penetration velocity (u) for hydrogels RK_1 to RK_8 having varying AA content in feed. The values of K_r and u are reported in Table III. Figure 6 shows that u increased with increasing AA content from 33.34–75%, whereas K_r decreased (swelling rate increases) indicating a higher affinity for water. Because an increase in AA content provides the increased polymer chain relaxation to increase the free volume through which media can travel. Thus, specific interaction between the hydrogel network and the medium is stronger, and hydrogels swell faster.

However, when AA content was further increased up to 80% (RK_5), u slightly decreased, but K_r increased. As for RK_5 hydrogel, 80% AA content was taken in feed, but for this case, only 70% AA content was incorporated in resulting hydrogel RK_5, leading to incorporation of higher AM content and HEA content, as given in Table II. According to the above reason, crosslink density may be increased, as shown in SEM of RK_5 hydrogel [Figure 4 (c)], which indicates a denser network of the hydrogel. For RK_5 to RK_8 hydrogels when AA content increased from 80 to 93.76%, u nominally further increased, but K_r decreased, leading to again increased affinity for water. Therefore, it could also be expected from Figure 6 that as AA content increased for RK_1 to RK_8 hydrogels, both media penetration velocity and swelling rate (i.e., inverse of K_r) increased in similar trend as followed in equilibrium swelling ratio depending on AA content. Thus, swelling rate and media penetration velocity are governed by both the factors, i.e., equilibrium swelling ratio and AA content. The swelling kinetic results obtained were different than those of poly(acrylamide-*co*-acrylic acid) hydrogel[5] in which only increasing trend in swelling kinetic was observed when AA content increased from 7.3 to 29.1 mol %. Katime et al.[24] had observed media penetration velocity for poly(AM-*co*-AA) hydrogel in the range of 4.02×10^{-5}–2.87×10^{-5}.

Effect of AA on the network parameter study

To verify the effect of incorporated AA content on hydrogel structure and dynamic swelling behavior, we determined the network parameter such as average molecular weight between crosslinks (M_c), mesh size (ξ), and crosslink density (q) for hydrogels RK_1

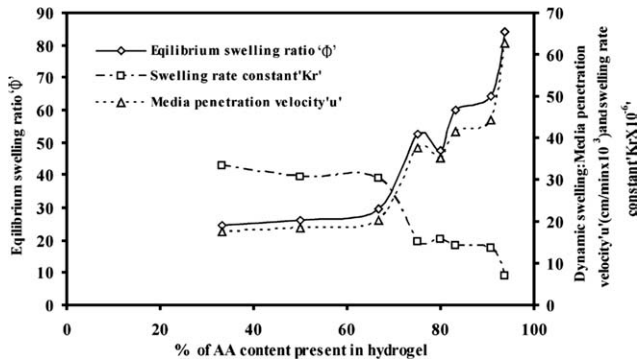

Figure 6 Effect of acrylic acid content on equilibrium swelling ratio, swelling rate constant, and media penetration velocity of poly(AM-*co*-AA-*co*-HEA) hydrogels comprised of 33.34%–93.76% acrylic acid (AA) content.

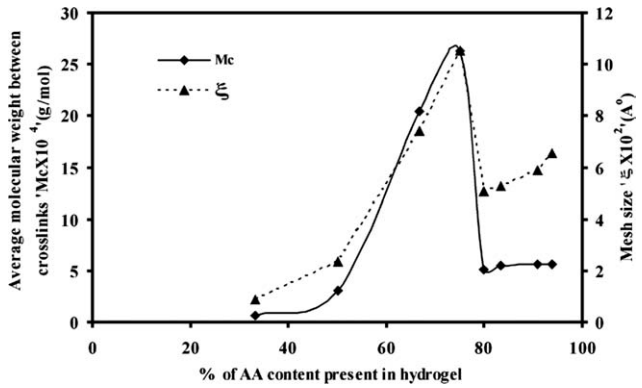

Figure 7 Effect of acrylic acid content on average molecular weight between crosslinks and mesh size of poly(AM-*co*-AA-*co*-HEA) hydrogel comprised of 33.34%–93.76% acrylic acid (AA) content.

to RK_8 having varying AA content. The network parameters were determined for RK_1 to RK_8 hydrogels using eqs. (7), (8), and (10), respectively. The results are listed in Table III. From the network parameters study, it is indicated that a decrease of molecular weight between crosslinks (M_c) and mesh size (ξ) is accompanied by an increase of crosslink density (q), resulting in a decrease of swelling ratio. The effect of AA content on mesh size (ξ) and molecular weight between crosslinks (M_c) for RK_1 to RK_8 hydrogels is shown in Figure 7. The solid curve with (◆) represents the values of molecular weight between crosslinks (M_c), and dotted line curve with (▲) is used to present mesh size (ξ). Figure 8 shows the plot between crosslink density and AA content. It is clear from Figure 7 that the molecular weight between crosslinks (M_c) drastically increased from 6.54×10^3 to 2.63×10^5 and mesh size (ξ) increased from 8.70×10^1 to 1.05×10^3 when the AA content increased from 33.34% (RK_1) to 75% (RK_4) in feed. In the same fashion, crosslink density decreased from 3.31×10^{-2} to 3.60×10^{-4}, as shown in Figure 8. These results may be attributed to the fact that higher AA content[37] contributed to the formation of greater chain length, producing hydrogel networks with lower crosslink densities and higher average molecular weight between two consecutive crosslinks. Therefore, increased repulsion force of the carboxylate groups provides enlarge mesh size during the swelling. Accordingly, RK_1 to RK_4 hydrogels exhibited higher swelling ratio, media penetration velocity, as well as swelling rate.

As discussed earlier, for RK_5 hydrogel, only 70% AA content was incorporated in resulting hydrogel, which was comparatively very low than those in feed having 80% AA. This leads to exceptionally high AM content and higher HEA content in resulting hydrogel RK_5. This difference between feed and resulting chemical composition impacted the structure of hydrogel RK_5, as shown in SEM of RK_5 hydrogel, which leads to more pronounced roughness of the surface with somewhere very few bead-like formation. The increased AM content[34] and higher HEA[38] content lead to not only a decrease in the repulsion force of the carboxylate groups due to the decrease of AA content in hydrogel network but also a decrease in the network repulsion volume. This explanation could be verified by the network parameters. From Figure 7, it is clear that when the AA content further increased up to 80% (RK_5) in feed, exceptionally the M_c dropped down from 2.63×10^5 to 5.12×10^4 and ξ decreased from 1.05×10^3 to 5.06×10^2. For this case, Figure 8 reveals that crosslink density increased from 3.60×10^{-4} to 1.69×10^{-3} demonstrating its rigid network of higher crosslink densities. With such a large degree of physical restriction in the hydrogel network RK_5, water uptake decreased markedly. These results confirm that the observed low swelling ratio in the resulting hydrogel RK_5 was due to the increased crosslink density created by the incorporation of lower AA content and increased AM as well as HEA content. Thus, these results show good agreement with SEM of RK_5 hydrogel, and therefore, lower swelling ratio, media penetration velocity, as well as swelling rate.

Moreover, Figure 7 shows further nominal increase in M_c from 5.12×10^4 to 5.68×10^4 and increase in ξ from 5.06×10^2 to 6.55×10^2 until the AA content increased up to 93.76% (RK_8). As a result, crosslink density decreased from 1.69×10^{-3} to 1.35×10^{-3} (Fig. 8), which leads to porous and granular structure for RK_5 to RK_8 hydrogel. These results were in accordance with SEM for RK_7 and RK_8 hydrogels, respectively [Figures 4 (d,e)], which exhibit smaller grain size and more porous structure leading to higher swelling ratio with increasing AA content. Therefore, increased AA content was further responsible for increased equilibrium swelling ratio,

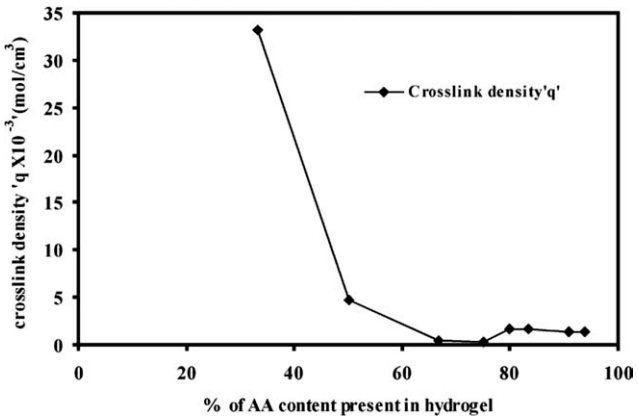

Figure 8 Effect of acrylic acid content on crosslink density of poly(AM-*co*-AA-*co*-HEA) hydrogel comprised of 33.34%–93.76% acrylic acid (AA) content.

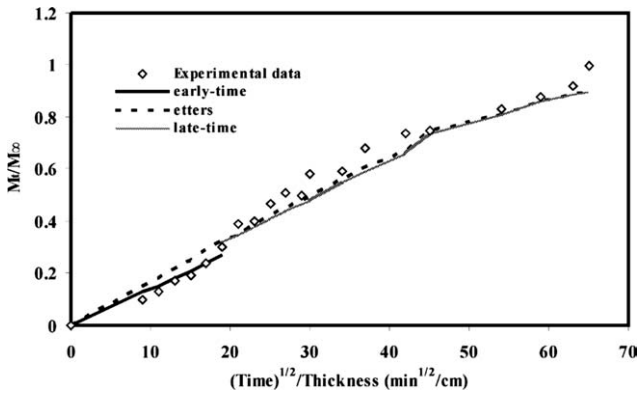

Figure 9 Diffusion model fits for the early-time, late-time, and Etters approximations of Fickian diffusion through the thin disk for designated hydrogel RK1: (1/1/1).

media penetration velocity, as well as swelling rate. Therefore, it can be expected that network parameters result affected the dynamic swelling parameter. Jovanovic et al.[15] had reported that an increase in the molar mass between crosslinks (M_c) and the distance between the macromolecular chains (ξ) leads to an increase in the values of swelling kinetic parameters, whereas an increase in the crosslink density (q) showed the opposite effect for poly (acrylic acid) hydrogel by varying the crosslinker/monomer ratio in the range of 0.003–0.010 mol.

Effect of AA on modeling of the diffusion process

The values of early diffusion coefficient (D_i), late diffusion coefficients (D_L), and Etters diffusion coefficients (D_E) were calculated according to eqs. (13), (14), and (15) respectively, for hydrogels RK_1 to RK_8, and the results are shown in Table III. Very low value of standard deviation, i.e., 10^{-4}–10^{-5} in the Ds values for each hydrogels in every diffusion model, shows that there is no variation in hydrogel composition, and the three Ds calculated for each hydrogel in every diffusion model were statistically equivalent. A plot between (M_t/M_∞) versus $t^{1/2}$ for all hydrogels was plotted, and slope was determined and substituted in eq. (13) to obtain early diffusion coefficient (D_i). The late diffusion coefficient (D_L) in eq. (14) was determined from slope of plot between ln $[1-(M_t/M_\infty)]$ versus t. The slope of linear plot between ln $[1-(M_t/M_\infty)^b]$ versus t^a was used for the evaluation of Etters diffusion coefficients (D_E) in eq. (15). By using these values of D_i, $D_{L,}$ and D_E diffusion coefficients, the fractional solvent absorbed (M_t/M_∞) was calculated at different time intervals from "early" time, late-time, and "Etters" diffusion model as described in eqs. (13), (14) and (15) respectively. Subsequently, the calculated (M_t/M_∞) values at different time intervals were fitted into the experimental data in plot of (M_t/M_∞) against $(\text{time})^{1/2}$/thickness. The examples of fitting of these three models into the experimental value are shown in Figure 9 for RK_1 and Figure 10 for RK_8 hydrogels. In the fitting of early-time, late-time, and "Etters" diffusion models into the experimental data, the calculated value of (M_t/M_∞) is shown by (—) thick line for early time, (| | |) firm line for late time, and (- - - - -) dotted line for Etters model; while experimental fractional solvent absorbed (M_t/M_∞) value is shown by (□) point. The early-time, late-time, and "Etters" diffusion models fitted to the experimental data exhibited that the diffusion rate of water uptake through these hydrogels was primarily Fickian in nature. The values of the transport/diffusion exponent ($n = 0.5$) show good agreement with fitting of these models to the experimental data. The similar results have been previously observed by Mullarney[11] for the pheniramine maleate (PM) drug diffusion in copolymers of *N*,*N*-dimethylacrylamide modified with hydrophobically 2-(*N*-ethylperfluorooctanesulfonamide) ethylacrylate (FOSA) by varying the FOSA monomer in the range of 0–72%.

It was exhibited from Figure 9 that for RK_1 hydrogel containing 33.34% AA content early model was applicable for first 30% water absorption, as shown by (—) thick line, and deviate after 30% water absorption, and here begins working of late model, which was applicable for latter 70% water absorption, as shown by (| | |) firm line. Similar trend of applicability range of early model and late model for water absorption was followed in all hydrogel RK_2 to RK_7 having different AA content from 50 to 90.90%, whereas in the case of RK_8 hydrogel containing highest AA content, i.e., 93.76%, early model is valid for first 50% water absorption and late model is valid for latter 50% water absorption. The Etters model is valid up to full range of water absorption, i.e., 1–100% for all sample of hydrogel [Figures 9

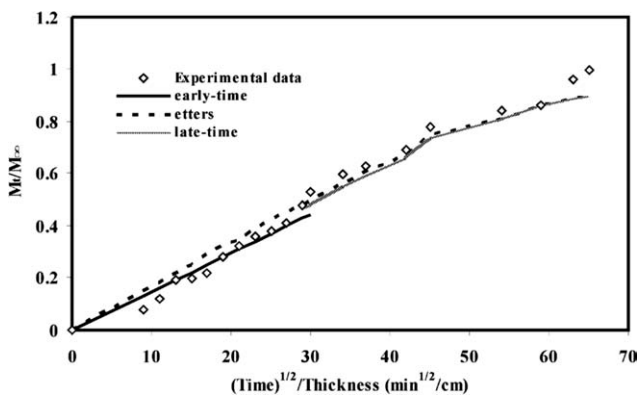

Figure 10 Diffusion model fits for the early-time, late-time, and Etters approximations of Fickian diffusion through the thin disk for designated hydrogel RK8: (1/30/1).

and 10]. It is also clear from Figure 10 that the highest AA content in RK_8 hydrogel not only increases the swelling capacity but also has a significant effect on the diffusion kinetic of swelling.

Generally, rank of diffusion coefficients was followed in the order of late time > Etters > early time. Therefore, it can be expected that the solution proposed by Etters "smoothed" the transition in the profile between the early- and late-diffusion times. From the value of diffusion coefficients for these three models as shown in Table III, It is clear that the diffusion coefficients were higher when the hydrogel was in its more hydrated form (i.e., at later times), and the water absorption could diffuse more quickly through the increased volume of the hydrophilic phase. The early-time diffusion coefficient values ranged from 4.42×10^{-5} to 3.79×10^{-5} cm^2/min. The Etters diffusion coefficients ranged from 7.21×10^{-5} to 5.33×10^{-5} cm^2/min. The late-time diffusion coefficients ranged from 8.11×10^{-5} to 5.07×10^{-5} cm^2/min. Typical diffusion coefficient values for water diffusion in these hydrogels were in the order of 10^{-5} cm^2/ min; therefore, diffusion through these hydrogels was generally rapid. In these experiments, there was no significant change in the diffusion coefficients between the early-time, late-time, and Etters for a given experimental condition, suggesting that water absorption rate was generally constant.

CONCLUSIONS

The following conclusions can be made from the study of the chemically crosslinked poly(acrylamide-*co*-acrylic acid-*co*-2-hydroxy ethyl actylate) [AM-*co*-AA-*co*-HEA] hydrogel

1. Elemental analysis showed that higher AM was incorporated in resulting hydrogel than AM taken in feed. Residual AA estimation analysis showed that approximately same AA content was being incorporated in all resulting hydrogel as taken in feed, except for hydrogel containing 80% AA content in feed. HEA was incorporated in lower amount in synthesized hydrogel.
2. Because of the above reason, equilibrium swelling ratio decreased for hydrogel containing 80% AA in feed. Although swelling ratio increased nearly fourfold from 24.52 to 85.22 as the AA was increased from 33.34 to 93.76%.
3. Network parameter study showed that molar mass between crosslinks and mesh size followed an increasing trend for swelling ratio with increasing AA. Also, similar trend for media penetration velocity and swelling rate was observed.
4. Swelling data fitted to early-time, late-time, and Etters diffusion models showed that diffusion rate of water uptake was primarily Fickian in nature. For hydrogels up to 90.90% AA content, the early model was applicable for first 30% water absorption and the late model was applicable for latter 70% water absorption. However, hydrogel containing excessive AA content (93.76%) did not follow the above trend, indicating deviation for extremely high AA-containing hydrogel. In this case, the early model was extended up to first 50% of water absorption, and the late model validity was contracted for latter 50% water absorption.
5. The Etters model was best applicable to all hydrogels as it is valid up to full swelling range.

Thus, it can be summed up that hydrogel composition, network parameters, and morphology play a significantly important role in controlling the swelling properties of ionizable hydrogels.

The authors thank Dr. R. K. Khitoliya, director H.B.T.I., Kanpur, for moral support and also gratefully acknowledge The Head, A.C.M.S., and Mrs. Beena, IIT Kanpur, for SEM analysis and recording the FTIR spectra, and Dr. D.K. Dixit, The Head, S.A.I.F., C.D.R.I., Lucknow, for elemental analysis.

References

1. Buyanov, A. L.; Gofman, I. V.; Revel'skaya, L. G.; Khripunov, A. K.; Tkachenko, A. A. J Mech Behav Biomed Mater 2010, 3, 102.
2. Kumar, A.; Srivastava, A.; Galaev, I. Y. Polym Sci 2007, 32, 1205.
3. Ganji, F.; Vasheghani-Farahani, E. Iran Polym J 2009, 18, 63.
4. Bajpai, A. K.; Shukla, S. K.; Bhanu, S.; Kankane, S. Prog Polym Sci 2008, 33, 1088.
5. Turan, E.; Caykara, T. J Appl Polym Sci 2000, 2007, 106.
6. Adnadjevic, B.; Jovanovic, J. J Appl Polym Sci 2008, 107, 3579.
7. Serra, L.; Domenech, J.; Peppas, N. A. Biomaterials 2006, 27, 5440.
8. Brazel, C. S.; Peppas, N. A. Polymer 1999, 40, 3383.
9. Arifin, D. Y.; Lee, L. Y.; Wang, C. H. Adv Drug Delivery Rev 2006, 58, 1274.
10. Weibull, W. J Appl Mech 1951, 18, 293.
11. Mullarney, M. P.; Seery, T. A. P.; Weiss, R. A. Polymer 2006, 47, 3845.
12. Guo, Q.; Knite, P. T.; Mather, P. T. J Controlled Release 2009, 137, 224.
13. Etters, J. N. Text Chem Color 1980, 12, 140.
14. Korsmeyer, R. W. Polymers for Controlled Drug Delivery; CRC Press: Boca Raton, 1991; p 16.
15. Jovanovic, J.; Adnadjevic, B. Polym Bull 2007, 58, 243.
16. Ferrer, G. G.; Sanchez, M. S.; Rebelles, J. L. G.; Colomer, F. J. R.; Pradas, M. M. Eur Polym J 2007, 43, 3136.
17. Singh, T. R. R.; McCarron, P. A.; Woolson, A. D.; Donnellt, R. F. Eur Polym J 2009, 45, 1239.
18. Peppas, N. A.; Hilt, J. Z.; Khademhosseini, A; Langer, R. Adv Mater 2006, 18, 1345.
19. Bundela, H.; Bajpai, K. Express Polym Lett 2008, 2, 201.

20. Turan, E.; Demirci, S.; Caykara, T. J Polym Sci Part B: Polym Phys 2008, 46, 1713.
21. Emileh, A.; Vasheghani-Farahani, E.; Imani, M. Eur Polym J 2007, 42, 1437.
22. Gupta, I.; Tomar, R. S.; Nagpal, A. K.; Singhal, R. J Macromol Sci Part A: Pure Appl Chem 2007, 44, 1.
23. Gudeman, L. F.; Peppas, N. A. J Appl Polym Sci 1995, 55, 919.
24. Katime, I.; Novoa, R.; Diaz de Apodaca, E.; Mendizabal, E.; Puig, J. Polym Test 1999, 18, 559.
25. Zhao, Y.; Chen, W.; Yang, Y.; Yang, X.; Xu, H. Colloid Polym Sci 2007, 285, 1395.
26. Tokuhiro, T.; Tokuhiro, A. T. Polymer 2008, 49, 525.
27. Liu, Y.; Velada, J. L.; Huglin, M. B. Polymer 1999, 40, 4299.
28. Tripathy, T.; Sing, R. P. Eur Polym J 2000, 36, 1471.
29. Vazquez, B.; Roman, J. S.; Peniche, C.; Cohen, M. E. Macromolecules 1997, 30, 8440.
30. Wang, H.; Wang, Z.; Zhu, B. React Funct Polym 2007, 67, 225.
31. Ritger, P. L.; Peppas, N. A. J Controlled Release 1987, 5, 37.
32. Ritger, P. L.; Peppas, N. A. J Controlled Release 1987, 5, 23.
33. Lee, J. W.; Kim, S. Y.; Kim, S. S.; Lee, Y. M.; Lee, K. H.; Kim, S. J. J Appl Polym Sci 1999, 73, 113.
34. Gupta, I.; Tomer, R. S.; Nagpal, A. K.; Singhal, R. Des Monomers Polym 2006, 9, 589.
35. Katime, I. A.; Katime, O.; Katime, D. Smart Materials of This Millenium: Macromolecular Hydrogels (in Spanish). Servicio Editorial de la Universidad del Pais Vasco: Bilbao, 2004.
36. Peppas, N. A.; Franson, N. M. J Polym Sci: Polym Phys Ed 1983, 21, 983.
37. Davison, G. W. R.; Peppas, N. A. J Controlled Release 1986, 3, 259.
38. Flory, P. J. Principal of Polymer Chemistry; Cornell University, Ithaca Press: New York, 1953.
39. Okay, O.; Durmaz, S. Polymer 2002, 43, 1215.
40. Hariharan, D.; Peppas, N. A. Polymer 1996, 37, 149.
41. Xue, W.; Champ, S.; Huglin, M. B. Polymer 2001, 42, 3665.
42. Peppas, N. A.; Merill, E. W. J Polym Sci Part A: Polym Chem 1976, 14, 441.
43. Crank, J. Diffusion in a Plane Sheet, the Mathematics of Diffusion; Oxford University: London, 1975; p 47.